AD-A078 027 NAVAL RESEARCH LAB WASHINGTON DC F/G 18/3
CROSS FIELD JETTING OF ENERGETIC IONS PRODUCED BY RAYLEIGH-TAYL--ETC(U)
OCT 79 S H BRECHT , K PAPADOPOULOS
UNCLASSIFIED NRL-MR-4068 NL

| OF |
AD
A078027

END
DATE
FILMED
1-80
DDC

NRL Memorandum Report 4068

Cross Field Jetting of Energetic Ions Produced by Rayleigh-Taylor Instability

S. H. BRECHT

Science Applications, Inc.
McLean, Virginia

AND

K. PAPADOPOULOS

Plasma Physics Division

October 3, 1979

This research was sponsored by the Defense Nuclear Agency under Subtask Code S99QAXHC047, work unit 15 and work unit title Debris Injection.

NAVAL RESEARCH LABORATORY
Washington, D.C.

SECURITY CLASSIFICATION OF THIS PAGE (When Data Entered)

REPORT DOCUMENTATION PAGE

READ INSTRUCTIONS BEFORE COMPLETING FORM

1. REPORT NUMBER: NRL Memorandum Report 4068
2. GOVT ACCESSION NO.:
3. RECIPIENT'S CATALOG NUMBER:

4. TITLE (and Subtitle): CROSS FIELD JETTING OF ENERGETIC IONS PRODUCED BY RAYLEIGH-TAYLOR INSTABILITY
5. TYPE OF REPORT & PERIOD COVERED: Interim report on a continuing NRL problem.
6. PERFORMING ORG. REPORT NUMBER:

7. AUTHOR(s): Brecht, K. Papadopoulos
8. CONTRACT OR GRANT NUMBER(s):

9. PERFORMING ORGANIZATION NAME AND ADDRESS: Naval Research Laboratory, Washington, DC 20375 — PE 62704H
10. PROGRAM ELEMENT, PROJECT, TASK AREA & WORK UNIT NUMBERS: NRL Problem 67H02-53; DNA Subtask S99QAXHC047

11. CONTROLLING OFFICE NAME AND ADDRESS: Defense Nuclear Agency, Washington, DC 20305
12. REPORT DATE: October 3, 1979
13. NUMBER OF PAGES: 34

14. MONITORING AGENCY NAME & ADDRESS (if different from Controlling Office):
15. SECURITY CLASS. (of this report): UNCLASSIFIED
15a. DECLASSIFICATION/DOWNGRADING SCHEDULE: 30 Oct 79

16. DISTRIBUTION STATEMENT (of this Report)

Approved for public release; distribution unlimited.

NRL-MR-4068

17. DISTRIBUTION STATEMENT (of the abstract entered in Block 20, if different from Report)

18. SUPPLEMENTARY NOTES

This research was sponsored by the Defense Nuclear Agency under Subtask Code S99QAXHC047, work unit 15 and work unit title Debris Injection.

19. KEY WORDS (Continue on reverse side if necessary and identify by block number)

Rayleigh-Taylor instability
Debris transport
Cross-field transport
Trapped betas

20. ABSTRACT (Continue on reverse side if necessary and identify by block number)

The phenomena of cross field jetting of debris following a nuclear detonation is explained by the Rayleigh-Taylor instability. The growth rate for the mode is calculated as well as thresholds for onset and wavelength. A model for this phenomena is developed and the amount of debris transported across the field lines is estimated.

DD FORM 1 JAN 73 1473 EDITION OF 1 NOV 65 IS OBSOLETE
S/N 0102-014-6601

SECURITY CLASSIFICATION OF THIS PAGE (When Data Entered)

251 950

TABLE OF CONTENTS

CROSS FIELD JETTING OF ENERGETIC IONS PRODUCED BY RAYLEIGH–TAYLOR INSTABILITY

I. Introduction

A high attitude nuclear explosion (HANE) can lead to cross field transport of debris which in turn produces energetic trapped betas on L shells considerably higher than the one on which the detonation took place. The jetting model currently used in the SPECTER code is an estimate from ad hoc arguments. In this work the cross field transport of charged debris, during expansion of the debris sphere, is modeled by considering the Rayleigh-Taylor instability in a linear calculation. The model considers three phemonena. Two provide energy sources for the instability and the third provides a damping mechanism. The damping mechanism allows estimates of minimum wavelengths for the modes as well as critical thickness and temperatures for onset of the instability.

The first phenomenom which can initiate the Rayleigh-Taylor instability is the laminar like accelerations of a percentage of the ions within the shock[1]. Essentially this leads to a three species description of the plasma. Particle simulations of an advancing shock have demonstrated the existence of these accelerated ions which have densities of approximately 10% of the ion density in the shock. The third species causes a space charge with the resultant electric field. The result of this is the Rayleigh-Taylor instability. The second source of energy for the instability is the curvature of the magnetic field lines caused by the bubble expansion. This force is more apparent during early phases of the bubble evolution. Finally, there is damping of the instability provided by finite Larmor radius corrections to the momentum equations (i.e. magnetic viscosity). The damping is a

Note: Manuscript submitted June 25, 1979.

function of the instability wavelength and is directly coupled to the thickness of the debris shell as well as the perpendicular pressure of the debris.

In this report a simplified model for prediction of these effects will be presented. Details of the calculation of all three phenomena are discussed in Appendix A and B and some sample estimate of growth rates, wavelengths and mass transport are presented in Appendix C.

II. Model

In this model we make use of the growth and damping rates represented by Eq. A-21 and Eqs. B-9, 10, 11. Use is also made of some scaling relations provided by Dr. Robert Clark. These relations have been previously provided under this contract. As in Appendix B, we work in cylindrical coordinates where the B field is in the $\tilde{\theta}$ direction and displacements are in the $\hat{r}$ and $\hat{z}$ direction, Fig. 1.

The growth rate from the laminar acceleration is represented by the following equations

$$\gamma_L = k_z V_A \left(\frac{f}{2L_n L_m (k_z^2 - 1/L_n^2)} \right)^{\frac{1}{2}} \qquad \text{II-1}$$

where $L_n^{-1} \equiv \left|\frac{n_o'}{n_o}\right|, \left|\frac{\rho_o'}{\rho_o}\right|$, $L_m^{-1} \equiv \left|\frac{B_o'}{B_o}\right|$, V_A is the Alfven speed and f is the fraction of ions accelerated in the shock, typically 10%. In this report L_n is taken equal to L_m. Equation II-1 provides one of the restrictions on λ_z,

$$\lambda_z < 2\pi L_n \, . \qquad \text{II-2}$$

It should also be noted that as $\lambda_z \to o, \gamma_L \to$ constant. The damping rate

produced by finite larmor radius effects is calculated in Appendix B. and is found to be

$$\gamma_D = -\frac{3}{2}\frac{p_\perp k_r k_z}{\rho_o \omega_{ci}} \quad . \qquad \text{II-3}$$

The growth rate due to the centrifugal acceleration, calculated in Appendix B, is represented by one of two relations:

$$\gamma_{cI} = \left(\frac{k_r T_\perp}{2m_i}\ \frac{1}{L_n}\right)^{\frac{1}{2}} \qquad \text{II-4}$$

or if $(B_o')^2 > \dfrac{4\pi \rho_o k_r T}{L_n}$ or $1 > \dfrac{4\pi \rho_o k_r T_\perp L_m^{\,2}}{B_o^{\,2} L_n}$

$$\gamma_{cII} = \tfrac{1}{2}\frac{B_o}{L_m}\left(\frac{1}{\rho_o \pi}\right)^{\frac{1}{2}} \qquad \text{II-5}$$

Equations II-1,3,5 lead to estimate of the minimum wavelength in the z direction ie: the condition for growth is

$$\gamma_L + \gamma_c > \gamma_D, \qquad \text{II-6}$$

Where Eq. II-5 is the limit most likely to occur in this problem, using equations II-1, II-3, and II-5, one obtains the following relation

$$\frac{V_A}{L_n}\left[\left(\frac{\rho_A}{\rho_o}\right)^{\frac{1}{2}} + \left(\frac{f}{2}\right)\right] > \frac{3}{2}\ \frac{p_\perp k_r k_z}{\rho_o \omega_{ci}} \quad , \qquad \text{II-7}$$

or

$$\lambda_z > \frac{12\pi^2 L_n k_r p_\perp V_A \rho_A}{B_o^{\,2}\omega_{ci}\left[\left(\frac{\rho_A}{\rho_o}\right)^{\frac{1}{2}} + (f/2)^{\frac{1}{2}}\right]\rho_o}. \qquad \text{II-8}$$

Equation II-2 and II-8 provide the upper and lower bound on λ_z. One additional condition is required to complete the discription that is $\lambda_z < \pi R$. This implies that the wavelength must be less than the upper half of the circumference of the bubble. These three conditions determine the time of onset for the instability and provide additional information as to possible orientation of region of maximum instability.

The next estimate required is the amount of mass involved in the instability. If we consider a typical sinusoidal oscillation as the perturbation, an estimate of amount of debris can be achieved. See figure 2.

If $\zeta_r < \lambda/4$ and $\lambda/4 < R$ we can assume angles θ and ϕ small and arrive at the following relation

$$\zeta_r \sim \frac{\lambda_z^2}{16R} \quad , \qquad \text{II-9}$$

where ζ_r must be less than Δ, the coupling shell thickness. In order for the instability to remain in the linear regime it has been shown[2] that $\zeta_r < .2\lambda_z$. We will take $\zeta_r \sim .1\,\lambda_z$. As the instability progresses into the nonlinear regime most of the mass involved can be reasonably estimated by the area within the linear regime. The area subtended by a triangle which covers the ejected mass regions of a single oscillation is approximately

$$A \sim \tfrac{1}{4}\,\lambda_z \zeta_r \sim \frac{\lambda_z^2}{40} \qquad \text{II-10}$$

The total mass ejected per lobe is then estimated by $\rho_o A \ell_\theta$ and the total

number of debris particles is estimated by

$$D_T \approx n_D A \ell_\theta . \qquad \text{II-11}$$

The scale length, ℓ_θ, is considered to be the wavelength in the $\hat{\theta}$ direction. Since the Rayleigh-Taylor instability is a flute type mode typically $\underline{k} \cdot \underline{B} \approx 0$, however there can be finite $k_{||}$ or in this case k_θ as long as $k_{||}/k_\perp < (m_e/m_i)^{\frac{1}{2}}$. This establishes an upper bound on ℓ_θ. A lower bound is approximately half the hemispheric distance in the $\hat{\theta}$ direction so the minimum $\ell_\theta = \frac{\pi R}{2}$. Here we will take the conservative estimate $\ell_\theta = \lambda_\theta = \frac{\pi R}{2}$. The volume of debris involved in each outward jetting lobe can now be calculated from Eq. II-11.

The scaling used in this model was obtained from numerical calculations by Dr. Robert Clark. We begin with the usual kinetic energy relation

$$Y_k = 1/2 \; M_o u_o^2 \qquad \text{II-12}$$

where Y_k is the kinetic yield in ergs.
Assuming complete coupling and $\rho_A(R) \sim$ const

$$M_o u_o = \left(M_o + \tfrac{4}{3} \pi R^3 \rho_A \right) u$$

more exactly $M_o u_o = (M_o + \lambda\pi \int_o^R R'^e \; \rho_A(R')dR')\, u$
If we define $R^{*3} \equiv M_o/(4/3 \; \pi \rho_A)$ as the radius at which a weapon mass of air is swept out then the following scaling appears:

$$u/u_o = 1/(1 + R^3/R^{*3}) \qquad \text{II-13}$$

$$\frac{M}{M_o} = 1 + R^3/R^{*3} \qquad \text{II-14}$$

$$u_o t = R(1 + 1/4\ R^3/R^{*3}) \qquad \text{II-15}$$

Making use of the marginal stability criterion for the ion-ion instability and assuming β_e is less than unity, a scaling relation can be derived for the B field in the shock as a function of radius

$$B_o \sim \frac{u(4\pi\rho_A)^{\frac{1}{2}}}{2.5}\ \alpha$$

Using Eq. II-13 we obtain the relation

$$B_o \sim \alpha\ u_o(4\pi\rho_A)^{\frac{1}{2}}/2.5(1 + R^3/R^{*3}) \qquad \text{II-16}$$

where $B_o \geq B_A$ must hold. This relation is an underestimate of the B field as the ion-ion instability has already begun. Comparisons with simulations show that a factor of 3 is necessary to bring this relation into agreement with the simulations. Therefore, the factor α is set equal to 3 in recognition of this fact.

The scaling of temperature is obtained by noting that $T_i < T_{kinetic}$ must hold because Landau damping for the ion-ion instability occurs where $V - V_A < \bar{V}_i \equiv \sqrt{\frac{kT_i}{m_i}}$. We then use the following scaling:

$$mu^2 \equiv kT_{kinetic}$$

$$(kT_i/m_i u^2) \sim .2$$

therefore $\qquad kT_i \sim .04\ m_i u^2 \sim .04\ kT_{kinetic} \qquad \text{II-17}$

Substituting Eqs. II-16, II-17, II-13 into Eq. II-8 we obtain

$$\lambda_z > \frac{12\pi^2 k_r L_n (.04) m_i u^2 \rho_A}{\omega_{ci} B_o (4\pi\rho_A)^{\frac{1}{2}} \left(\left(\rho_A/\rho_o \right)^{\frac{1}{2}} + (f/2)^{\frac{1}{2}} \right)}$$

or

$$\lambda_z > \frac{3\pi L_n k_r (.04)(2.5)^2}{\alpha^2 (4\pi\rho_A)^{\frac{1}{2}} \left(\left(\rho_A/\rho_o \right)^{\frac{1}{2}} + (f/2)^{\frac{1}{2}} \right)} \frac{m_i c}{e} \qquad \text{II-18}$$

This minimum wavelength can now be estimated if k_r and L_n are known. We estimate the maximum λ_r to be the coupling shell thickness, Δ, and estimate the density and magnetic scale lengths to be the e-folding distance of half the coupling shell thickness, $L_n \sim .37\ \Delta/2$. From simulations of Dr. Clark it is found that the coupling shell thickness with respect to the magnetic bubble radius varies with time. For reasons to be discussed in the following paragraph the instability will have its onset when approximately one weapon mass has been swept out. For Starfish the time at which $R = R^*$ is approximately 120 msec, at this time $\Delta \sim .025R$.

The estimate that the instability onset begins at approximately $R=R^*$ is determined by Eq. II-2. At this point in the dynamics a variety of effects appear but the dominant effects are the drop in temperature and continued increase in the coupling shell thickness allowing the condition on Eq. II-1 to be met. Applying this scaling for k_r and L_n, Eq. II-2 and Eq. II-18 can be written as

$$\lambda_z < 0.37\ \Delta/2 \qquad \text{II-19}$$

and

$$\lambda_z > \frac{6\pi^2(.37)(.04)(2.5)^2}{\alpha^2(4\pi\rho_A)^{\frac{1}{2}}\left[(\rho_A/\rho_o)^{\frac{1}{2}} + (f/2)^{\frac{1}{2}}\right]} \qquad \text{II-20}$$

An additional piece of information is also available from Eq. II-19. The coupling shell thickness is a function of angle with respect to the magnetic field approximated by

$$\Delta(R,\theta) = \Delta(R)/\sin\theta, \quad \theta > \theta_o$$

where θ_o is the angle at which coupling fails, $\theta_o \sim \sqrt{\Delta/R}$.

Equation II-19 provides the major restriction to the onset time of the instability. As can be seen, increasing Δ leads to earlier onset of the mode, therefore there will be a preferred direction to the largest modes. Since the field lines are frozen into the plasma and the instability is a flute instability $\underline{k}\cdot\underline{B} = 0$, the region of max. Δ, where the expansion is perpendicular to the frozen field line, will be some angle between field alignment, $\theta = 0$ and perpendicular to the ambient field line $\theta = \pi/2$, but will easily satisfy the condition $\theta > \theta$. For symmetrical expansion into a B field in a constant density atmosphere, one expects two regions of earliest onset, see Fig. 3. However, the atmosphere is exponential and therefore one has a preferred direction along the ambiant density gradient where Δ will actually be the largest, Fig. 4. This argument suggests that the region of maximum growth will be in a direction slightly southward and essentially upward for Starfish, Fig. 4. This model predicts onset of the Rayleigh-Taylor instability at a time when $R = R^*$. At this time the wavelength is estimated to be

$$\lambda_z > \frac{m_i c}{e} \frac{5.48}{\alpha^2(4\pi\rho_A)^{\frac{1}{2}}\left[(\rho_A/\rho_o)^{\frac{1}{2}} + (f/2)^{\frac{1}{2}}\right]} \qquad \text{II-21}$$

and the number of debris atoms injected is represented by

$$N_D = \frac{\pi^2 n_D \lambda_z R}{20} \ell_\theta \qquad \text{II-22}$$

Here n_D is taken to be $0.5\ (n_s)$ with $n_s \sim 4\ n_A$ where n_A is the ambient ion density, R is as usual the radius of the bubble and ρ_A is the ambient mass density of the ions. Generally all quantities labeled f_o are defined in the coupling shell and the ambient is defined to be the air located at the shock.

III. Summary

The Rayleigh-Taylor instability is found to be unstable with growth rates determined by Eqs. II-1,3,5 and wavelengths determined by II-2 and II-21. The wavelength and the total number of debris particles transported across the field lines, N_D, are found to be functions of altitude. The instability appears to onset when a weapon mass of air has been swept out by the expanding shock front. From considerations of the relative thickness, Δ, of the coupling shell a directional dependence can be surmised. The direction most optimal for the instability appears to be oriented in the direction of the ambient density gradient.

For the purpose of modeling the following relations appear to produce the appropriate results. The wavelength is

$$\lambda_z = \frac{5.48\ m_i c}{e\alpha^2 (4\pi\rho_A)^{\frac{1}{2}} \left[(\rho_A/\rho_o)^{\frac{1}{2}} + (f/2)^{\frac{1}{2}} \right]}$$

where $\alpha = 3$, ρ_o is the mass density in the coupling shell, $f = 0.1$, ρ_A is the ambient density at the coupling shell and $m_i = 27\ m_p$. The total number of debris

particles transported across the field lines is computed by the relation

$$N_D = \frac{\pi^2 n_D \lambda_z R}{20} \ell_\theta,$$

with $n_D = 0.5\, n_s$ where n_s is the density in the coupling shell and $n_s \sim 4\, n_A$ where n_A is the ambient mass density at the coupling shell altitude. The $\hat{\theta}$ scale length is taken to be $\ell_\theta = \pi R/2$ where $R \approx R^*$ and R^* is the radius at which one weapon mass of air has been swept out.

Appendix A. Linear Calculation of Rayleigh-Taylor Instability Driven by Shock Acceleration

In this calculation it is assumed that the shock is moving perpendicular to the magnetic field lines. The shock, spatial gradients and force are taken in the $\hat{z}$ direction with the magnetic field in the $\hat{y}$ direction. Three species are considered. The electrons and ions moving in the shock frame of reference and a third species comprising approx. 10% of the density, accelerated within the shock with a force $F = \frac{1}{2} \frac{m_2 V_A^2}{L_m}$, where V_A is the Alfven speed and, L_m is the magnetic field scale length. Further, it is assumed that the magnetic field is frozen into the plasma.

Five variables are unknown, the perturbed velocities for the two ion species and the three perturbed densities. Therefore, five equations are necessary. Consider the general momentum equation:

$$n_j m_j \frac{\partial \underline{v}_j}{\partial t} + n_j m_j (\underline{v}_j \cdot \underline{\nabla}) \underline{v}_j = q_j \frac{n_j}{c} \underline{v}_j \times \underline{B} + n_j q_j \underline{E} - \nabla \underline{P}_j + n_j \underline{F}_j \qquad \text{A-1}$$

and apply the following scaling $\omega_{ci} \gg \frac{\partial}{\partial t}, \underline{V} \cdot \underline{\nabla}$ and $\omega_{ce} \gg \omega_{ci}$. This implies that inertial terms can be neglected and that $\nu_{ei}/\omega_{ce} \ll \nu_{ie}/\omega_{ci}$. $\underline{F}_j$ represents collisional drag or acceleration depending on the species and is in the $\hat{z}$ direction. With this ordering the electron momentum Eq. becomes:

$$n_e q_e (\underline{E} + \underline{v}_e \times \frac{\underline{B}}{c}) - \nabla \underline{P}_e + n_e \underline{F}_e = 0 \qquad \text{A-2}$$

The ion momentum equation to lowest order in the cyclotron frequency becomes:

$$q_i \frac{n_i}{c}(\underline{v}_i \times \underline{B}) + n_i q_i \underline{E} - \nabla \underline{P}_i + n_i \underline{F}_i \text{ with } i = 1,2 \qquad \text{A-3}$$

so that the lowest order in velocity is:

$$\underline{v}_i^{(o)} = + c \frac{\underline{B} \times \nabla \underline{P}_i}{q_i n_i B^2} - c \frac{\underline{B} \times \underline{F}_i}{q_i B^2} \qquad \text{A-4}$$

To the next order one obtains

$$n_i m_i \left[\frac{\partial \underline{v}_i^{(o)}}{\partial t} + (\underline{v}_i^{(o)} \cdot \nabla) \underline{v}_i^{(o)} \right] = n_i q_i \left[\underline{E} + \frac{\underline{v}_i \times \underline{B}}{c} \right] - \nabla P_i + n_i \underline{F}_i \qquad \text{A-5}$$

In addition to Eqs. (A2 and 5) we use the continuity equation

$$\frac{\partial n_j}{\partial t} + \nabla \cdot (n_j \underline{v}_j) = 0 \qquad \text{A-6}$$

and the ideal gas assumption

$$P_j = n_j T_j \qquad \text{A-7}$$

We shall assume charge neutrality, $\nabla \cdot \underline{J} = 0$, and incompressibility, $\nabla \cdot \underline{v}_j = 0$. Further, we substitute $\underline{v}_i^{(o)}$ for $\underline{v}_i$ in the equations and then write $\underline{v}_i$ to represent $\underline{v}_i^{(o)}$. The assumption that $\underline{v}_i^{(o)}$ is equal to the $\underline{v}_i$ is valid if $\frac{c\underline{B} \times \underline{E}}{c} \gg \frac{c\underline{B} \times \nabla \underline{P}e}{n_e q_e B^2} - \frac{c\underline{B} \times \underline{F}_e}{q_e B^2}$ which is generally true. Therefore, Equation (A-6) becomes

$$\frac{\partial n_j}{\partial t} + \underline{v}_i \cdot \nabla n_j = 0 \qquad \text{A-8}$$

Adding Eqs. A-2 and 5 we obtain

$$n_i m_i \frac{d\underline{v}_1}{dt} + n_2 m_2 \frac{d\underline{v}_2}{dt} = (n_e q_e + n_1 q_1 + n_2 q_2)\underline{E} + (n_e q_e \underline{v}_e + n_1 q_1 \underline{v}_1 + n_2 q_2 v_2) x \frac{\underline{B}}{c}$$

$$- \nabla(P_e + P_1 + P_2) + n_e \underline{F}_e + n_1 \underline{F}_1 + n_2 \underline{F}_2 \qquad \text{A-9}$$

Recall that $\underline{\nabla} \cdot \underline{J} = 0$ implies that one can write

$$J = -\hat{e} \times \nabla\psi \qquad \text{A-10}$$

where ψ is a scaler potential function such that $J \times B = -\underline{B}\nabla\psi$.

Using Eq. (A-10) in Eq. (A-9) and making use of quasineutrality, we obtain

$$n_1 m_1 \frac{dv_1}{dt} + n_2 m_2 \frac{dv_2}{dt} = -\nabla\hat{P} + \Sigma_j n_j F_j \qquad \text{A-11}$$

where $\underline{\hat{P}} = \underline{P}_e + \underline{P}_1 + \underline{P}_2 + \underline{B}\psi$ and we have assumed this problem is electrostatic. At this point two ways to approach the problem are available either linearize Eq. A-11 as it stands using $f_1 = f_1 e^{i(\underline{k}\cdot\underline{x} - \omega t)}$ and keep fourier components in both directions, $\hat{x}$ and $\hat{z}$, or move to a center of mass of motion for the ion species and then linearize. If the first option is applied one must use energy conservation to close the set of equations. The result, to first order in k, is a complex cubic equation with complicated coefficients. The second method which will be followed here requires the following definitions:

$$V = \frac{\Sigma n_j m_j v_j}{\rho} \qquad \text{where} \quad \rho = \Sigma n_j m_j$$

, $\overline{F} = \Sigma_j n_j F_j$ and the perturbation takes the form $f(x\ z) = F(z)e^{i(k_x x - \omega t)}$.

Incompressibility is still required for the center of mass velocity as well as the individual ion velocities. Equation (A-11) becomes

$$\rho \frac{dV}{dt} = - \nabla\tilde{\rho} + \bar{F} \tag{A-12}$$

when $\nabla\cdot V = \nabla\cdot V_1 - \nabla\cdot V_2 = 0$ is used. Taking the curl of Eq. (A-12), and noting that V_o is in only the $\hat{x}$ direction since the calculation is done in the reference frame of shock moving in $\hat{z}$, and linearizing the resulting equation leads to

$$\rho_o \left\{ - ik_x \frac{dV_{1z}}{dt} + \frac{\partial}{\partial z} \frac{dV_{1x}}{dt} \right\} + \rho_o' \frac{dV_{1x}}{dt} = - ik_x F_{x-z} \tag{A-13}$$

Applying $\nabla\cdot V_1 = 0$ to equation (A-13) leads to a second order equation

$$\text{or} \quad \frac{\partial}{\partial z} \rho_o \frac{\partial V_{1z}}{\partial z} - k_x^2 \rho_o V_{1z} = - \frac{ik_x F_{x-1z}}{(\omega - k_x V_{ox})} \tag{A-14}$$

Since we are in the shock frame all accelerations on the shock are zero with the exception of those generated within the shock itself. The force on the second ion species is due to a type of laminar acceleration within the shock.[1] Therefore, the force term reduces to $F_{z1} = n_{21} F_2$. In order to proceed the force term is multiplied and divided by a factor of ρ, where the ratio of the perturbed density to the perturbed center of mass density is taken as zeroth order so that

$$\bar{F}_{z1} = n_{21} F_2 \rightarrow \rho_1 \frac{n_{21} F_2}{\rho_1} = \rho \tilde{F}_2.$$

Linearizing the center of mass continuity equation

$$\frac{\partial \rho}{\partial t} + \underline{V}\cdot\underline{\nabla}\rho = 0 \tag{A-15}$$

one obtains $-i(\omega - k_x V_{ox})\rho_1 + V_{1z}\rho_o' = 0$. Solving for ρ_1 and substituting into the force term one can rewrite Eq. (A-14)

$$\frac{\partial}{\partial z}\rho_o \frac{\partial}{\partial z} V_{1z} - k_x^2 \rho_o V_{1z} + \frac{k_x^2 \tilde{F}_o \rho_o' V_{1z}}{(\omega + k_x V_{ox})^2} = 0. \qquad \text{(A-16)}$$

The solution to this equation is easily obtain and has the form,

$$V_{1z} = e^{-\rho_o'/2\rho_o} e^{\pm iKz}$$

where

$$K^2 = \left(\rho_o'/\rho_o\right)^2 + \frac{F_o k_x \rho_o'/\rho_o}{(\omega - k_x V_{ox})^2} - k_x^2 .$$

The boundary conditions applied to the oscillatory portion of the solution, $q = e^{\pm iKz}$, leads to the quantization condition.

$$K^2 d^2 = n^2 \pi^2 \qquad \text{(A-17)}$$

where the boundary conditions are $q = 0$ at $z = 0$ and $q = 0$ and $z = d$. With z measured from the peak of the shock profile and d is the distance to the foot of the shock from $z = 0$. Using Eq. (A-17) leads directly to the equation

$$(\omega - k_x V_{ox}) = k_x \left(\frac{\tilde{F}_o \rho_o'/\rho_o}{\left(\frac{n\pi}{d}\right)^2 - \left(\frac{\rho_o'}{\rho_o}\right)^2 + k_x^2} \right)^{1/2} \qquad \text{(A-18)}$$

Now $\rho_o'/\rho_o = -1/\ell$ on the front side of the shock and there will be a growth rate from this mechanism if

$$k_x^2 + \left(\frac{n\pi}{d}\right)^2 > \left(\rho_o'/\rho_o\right)^2 = 1/\ell^2 \qquad \text{(A-19)}$$

If $(\frac{n\pi}{d})^2 > \frac{1}{\ell^2}$ the mode will become convective. One can then estimate the order of n that will allow the mode to grow. Since $\ell = de^{-1}$, then $n\pi < \frac{1}{.37}$ must be met. This means only the n = 0 terms will allow growing modes. Therefore, the wavelength of the instability must obey

$$\lambda_x < 2\pi\ell \ . \tag{A-20}$$

Providing this condition is met the growth rate becomes

$$\gamma = k_x V_A \left(\frac{\left|\frac{\rho_o'}{\rho_o}\right| f}{2L_m\left(k_x^2 - \left(\rho_o'/\rho_o\right)^2\right)} \right)^{1/2} , \tag{A-21}$$

where f is the fraction of accelerated ions and L_m the scale length of the magnetic field. In the cylindrical coordinates employed in the main body of this work $k_x \rightarrow k_z$.

Appendix B. Rayleigh-Taylor Instability Driven by Centrifugal Forces

To calculate the effects of centrifugal forces and the Larmor radius effect, it is necessary to work in cylindrical or spherical coordinates. For this problem cylindrical coordinates allows the necessary physics to be described; therefore, we will work in this system. Here we will work in Lagrangian with the various quantities described as follows:

$$\underline{B}_o = (0, B_\theta(R), 0) \quad R(t) = R(t_o) = \zeta(t)$$

$$\underline{U}_o(t_o) = \frac{R_o(t_o)}{\partial t} = 0 \quad \underline{u}_1(t) = \frac{\partial \underline{\zeta}(t)}{\partial t} = i\omega \underline{\zeta}$$

where $\underline{\zeta} = (\zeta_r, 0, \zeta_z)$ and $f_1 = f_1 e^{i(\underline{k} \cdot \underline{x} - (tot)}$

Four equations are necessary, we use: Faradays law

$$-\frac{1}{c}\frac{\partial \underline{B}}{\partial t} = \underline{\nabla} \times \underline{u} \times \underline{B} \text{ , where Ohms Law} \qquad \text{B-1}$$

$\underline{E} + \underline{u} \times B/c = 0$ has been used, the momentum equation

$$\rho \frac{\partial \underline{u}}{\partial t} = -\nabla \cdot \left(\underline{\underline{P}} + \frac{B^2}{8\pi} \right) + \frac{1}{4\pi} (\underline{B} \cdot \underline{\underline{\nabla B}}) + \frac{\underline{u} \times \underline{B}}{c} \qquad \text{B-2}$$

, the continuity equation

$$\frac{\partial n}{\partial t} + \nabla \cdot (n \underline{u}) = 0 \quad \text{where we assume } \underline{\nabla} \cdot \underline{u} = 0 \qquad \text{B-3}$$

and finally we assume for the pressure equation, the ideal gas law

$$\underline{P} = nT. \qquad \text{B-4}$$

Equations B-1,4 are now linearized. The off-diagonal pressure elements provide the finite Larmor radius effects. The off-diagonal pressure are represented in the following fashion,

$$\pi_{rr} - \pi_{zz} \sim \frac{P_\perp}{\omega_{ci}} \left[\frac{\partial u_z}{\partial r} + \frac{\partial u_r}{\partial z} \right] ,$$

$$\pi_{rz} \sim P_\perp / 2\omega_{ci} \left[\frac{\partial u_z}{\partial z} - \frac{\partial u_r}{\partial r} \right] , \qquad \text{B-5}$$

where $\pi_{zr} = \pi_{rz}$. The set of linearized equations consisting of two components of the momentum equation, Faradays law and the continuity equation are the placed in matrix form and the determinate set to zero to determine the frequency. After considerable algebra a dispersion relation accurate to the second order in k is obtained

$$\omega = - \frac{G \pm (G^2 - 4A)^{\frac{1}{2}}}{2} \qquad \text{B-6}$$

where $G = -\left(\frac{\beta}{\rho_o} - \frac{\delta \epsilon}{\rho_o(\rho_o - \kappa)}\right)$, $A = \alpha n_o'/\rho_o + \frac{1}{4\pi\rho_o}\left(\left(\frac{\partial B_o}{\partial r}\right)^2 - \left(\frac{B_o}{r}\right)^2\right)$

with $$\beta \equiv \frac{k_z P_\perp^\bullet}{\omega_{ci}} \left(3/r + \frac{1}{n_o}\frac{\partial n_o}{\partial r} - (3/2\ k_r)\right)$$

$$\delta \equiv \frac{P_\perp^\bullet k_r}{\omega_{ci}} \left(3/r + \frac{1}{n_o}\frac{\partial n_o}{\partial r}\right)$$

$$\alpha \equiv i\ T_\perp k_r$$

and

$$\epsilon \equiv - \frac{P_\perp}{2\omega_{ci}} \left(\left(1/r + \frac{1}{n_o}\frac{\partial n_o}{\partial r}\right)\ k_r - i k_r^2\right)$$

$$\kappa \equiv P_\perp^o/2\omega_{ci} \left(k_z \left(1/r + 1/r_o \frac{\partial n_o}{\partial r}\right) - k_r k_z\right) .$$

Neglecting terms of order $1/r^2$ and k^3

$$G \sim \frac{P_\perp^\bullet k_z}{\rho_o \omega_{ci}} \left(3/r + 1/r_o \frac{\partial n_o}{\partial r} - i\ 3/2\ k_r\right) \qquad \text{B-7}$$

Equation B-6 is in a form to be handled numerically since all of the components are either zeroth order terms or must obey scaling relations which have to be postulated to proceed any further.

The functional dependence of the growth rate for the wave can be obtained by approximating or expanding some of the components of Eq. B-16. For example, if one assumes the gyro-radius terms are smaller than the curvature term then

$$4A > G^2 \text{ or } (G^2 - 4A)^{\frac{1}{2}} \sim i2A^{\frac{1}{2}} \left(1 - G^2/8A\right)$$

and

$$\omega \sim -\frac{G}{2} \pm iA^{\frac{1}{2}} \left(1-G^2/8A\right) . \qquad \text{B-8}$$

The variable, A, can be approximated in three separate forms:

case 1
$$A^{\frac{1}{2}} \pm \frac{ik_r T_\perp n_o'}{\rho_o}^{\frac{1}{2}} \left[1 - \frac{i}{8\pi k_r T_\perp n_o'} \left(\left(\frac{\partial B_o}{\partial r}\right)^2 + \left(\frac{B_o}{r}\right)^2\right)\right]$$

case 2
$$A^{\frac{1}{2}} \sim \pm \frac{i\, B_o}{2r(\rho_o \pi)^{\frac{1}{2}}} \quad 1 - \frac{\left(\frac{\partial B_o}{\partial r}\right)^2}{\left(B_o/r\right)^2}$$

case 3
$$A^{\frac{1}{2}} \sim \pm \tfrac{1}{2} \frac{\partial B_o}{\partial r} \quad \frac{1}{(\rho_o \pi)^{\frac{1}{2}}} \quad \left(1 - \frac{B_o^2}{r^2 \left(\frac{\partial B_o}{\partial r}\right)^2}\right) .$$

Since G is complex there will be both a real frequency and a growth rate. The three cases lead to the following solutions:

case 1 ImA > ReA

$$\gamma \sim -\tfrac{3}{2} \frac{P_\perp}{\rho_o \omega_{ci}} k_r k_z \pm \left(\frac{k_r T_i}{2m_i} \left|\frac{n_o}{n_o}\right|\right)^{\frac{1}{2}} \left(1 + \frac{1}{8\pi k_r T_\perp n_o'} \left[B_o'^2 + \left(\frac{B_o}{r}\right)^2\right]\right) \qquad \text{B-9}$$

$$\omega \sim \frac{P_\perp k_z}{\rho_o \omega_{ci}} \left(3/r + n_o'/n_o\right) \mp \left(\frac{k_r T_\perp}{2m_i} \left|\frac{n_o'}{n_o}\right|\right)^{\frac{1}{2}} \left(1 + \frac{1}{8\pi k_r T_\perp n_o'} \left[B_o'^2 + \left(\frac{B_o}{r}\right)^2\right]\right)$$

case 2 $$\left(B_o/r\right)^2 > B_o'^2 > \text{ImA}$$

$$\gamma \sim -3/2\,\frac{P_\perp^{\,o}}{\rho_o \omega_i}\,k_r k_z \pm \frac{B_o}{2r}\left(\frac{1}{\rho_o \pi}\right)^{\frac{1}{2}}\left(\frac{2\pi k_r T_\perp n_o'}{B_o^{\,2}/r^2}\right)$$

B-10

$$\omega_r \sim 3/2\,\frac{P_\perp^{\,o} k_z}{\rho_o \omega_i}\left(3/r + \frac{n_o'}{n_o}\right) \mp \frac{B_o}{2r}\,\frac{1}{\rho_o \pi}^{\frac{1}{2}}\left(1 - \left(\frac{B_o'}{B_o/r}\right)^2\right)$$

case 3 $$\frac{B_o'^2}{B_o^{\,2}} > 1/r^2 > \frac{\text{ImA}}{B_o^{\,2}}$$

$$\gamma \sim -3/2\,\frac{P_\perp^{\,o}}{\rho_o \omega_i}\,k_r k_z \pm 1/2\,B_o'\left(\frac{1}{\rho_o \pi}\right)^{\frac{1}{2}}\left(1 - \left(\frac{B_o}{rB_o'}\right)^2\right)$$

B-11

$$\omega_r \sim \frac{P_\perp^{\,o} k_z}{\rho_o \omega_i}(3/r + n_o'/n_o) \mp B_o'\left(\frac{1}{\rho_o \pi}\right)^{\frac{1}{2}}\left(\frac{2\pi k_r T_\perp n_o'}{B_o'^2}\right)$$

As can be seen from these relations, the finite larmor radius terms provide a damping term and the curvature affects provide a growing term. For the work of current interest only case 1 or 3 are of interest. Typically case 3 appears to be the dominate limit.

Appendix C

Here we make an estimate of the various quantities derived in Sec. II of the report. We take the following parameters from calculations by Dr. Clark.

$n_i = 27mp$ $\qquad$ $\Delta \sim .025R$

$R \sim 220km$ $\qquad$ $n_i = 4n_A$

$f \sim 0.1$ $\qquad$ $n_i \sim 1 \times 10^6$

$n_A \sim 2.5 \times 10^5$ $\qquad$ $n_o \sim .5n_i$

$\rho_A \sim 6.68 \times 10^{-18}$ $\qquad$ $\rho_o \sim 4.5 \times 10^{-17}$

With these parameters we find the following sizes for the parameter. From Eq. II-21 we obtain

$$\lambda_z \sim 2.8 \times 10^6 \text{ cm} \quad \text{for } \alpha = 1$$

C-1

$$\lambda_z \sim 3.1 \times 10^5 \text{ cm} \quad \text{for } \alpha = 3$$

From Eq. II-22 the total number of debris atoms can be calculated using C-1.

$$N_D = \frac{\pi^2 n_D \lambda_z R \ell_\theta}{20} \sim 1.52 \times 10^{18} \ell_\theta \text{ , } \alpha = 3$$

C-2

$$N_D \approx 9.15 \times 10^{18} \ell_\theta \text{ , } \alpha = 1$$

Now C-2 can be completed if we know ℓ_θ. If we use

$$\ell_\theta = \lambda_\theta = \lambda_\perp \left(\frac{m_i}{m_e}\right)^{1/2}$$

then $\ell_\theta \sim 1.09 \times 10^8$. If we use $\ell_\theta \approx \pi R$ then $\ell_\theta \sim 6.97 \times 10^7$. Actually because of the effects of the exponential atmosphere in Δ as discussed in section II. We estimate $\ell_\theta \sim \pi R/2$ and use this as a lower bound on ℓ_θ. Then $\ell_\theta \sim 3.5 \times 10^7$ and

$$N_{D_{min}} \sim 5.3 \times 10^{25} \qquad \alpha = 3 \qquad \text{C-3}$$

$$N_{D_{max}} \sim 1.7 \times 10^{26} \qquad \alpha = 3 \qquad \text{C-4}$$

using the upper bound as ℓ_θ.

Using the result from C-1 the total number of wavelengths that will fit on the bubble is

$$N_w = \frac{\pi R}{\lambda_z} \sim 2.23 \times 10^2 \quad , \alpha = 3 \qquad \text{C-5}$$

$$N_w \approx 25, \quad \alpha = 1$$

The growth and damping rate have the following magnitudes. First we calculate some useful parameters

$$V_A \sim .3/(4\pi\rho_A)^{1/2} \sim 3.2 \times 10^7$$

$$R \sim R^*$$

$$u \sim u_o/2$$

$$u_o = \left(\frac{2Y_K}{M_o}\right)^{1/2} \sim 1.7 \times 10^8$$

$$B_o \sim \alpha u_o (4\pi\rho_A)^{1/2}/5$$

From Eq. II-1 and 5

$$\gamma_L + \gamma_{CH} \sim \frac{V_A}{L_n}\left[\left(\rho_A/\rho_o\right)^{1/2} + \left(\frac{f}{2}\right)^{1/2}\right] \sim 1.91 \times 10^2$$

From Eq. II-3

$$\gamma_D \sim -1.5\ (.04)\ u^2\ \frac{2\pi}{\Delta}\ \frac{2\pi}{\lambda_z}\ \frac{m_i c}{Be}$$

$$\gamma_D \sim -1.21 \times 10^2$$

$$\gamma = \gamma_D + \gamma_L + \gamma_C \sim 7.1 \times 10^1 \qquad \text{C-6}$$

This mode will e-fold quite rapidly after onset of the instability.

References

1. R. W. Clark, J. Denavit, and K. Papadopoulos, "Laminar Interactions in High Mach Number Plasma Flows: Phys. Fluids, 16, 1097, 1973.
2. John K. Dienes, "Method of Generalized Coordinates and an Application to Rayleigh-Taylor Instability", Phys. Fluids, 21, 736, 1978.

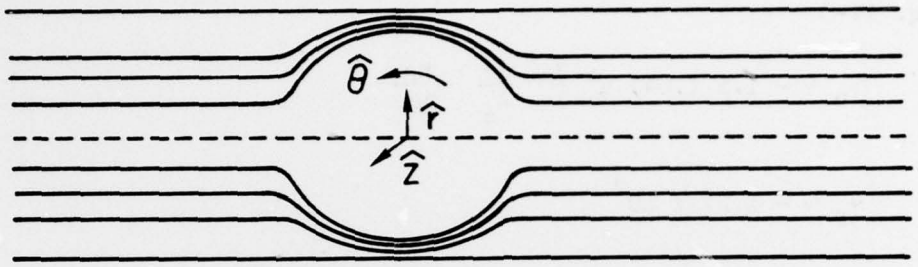

Fig. 1 - Coordinate system for the general calculation. In the bubble B = B(θ).

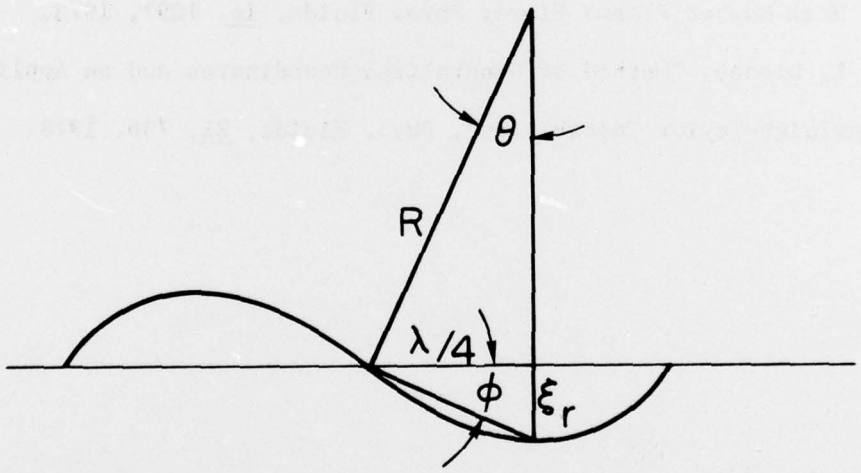

Fig. 2 - Linear deformation of the plasma surface during growth of Rayleigh-Taylor instability. ξ_r is the linear displacement, typically less than 20% of λ.

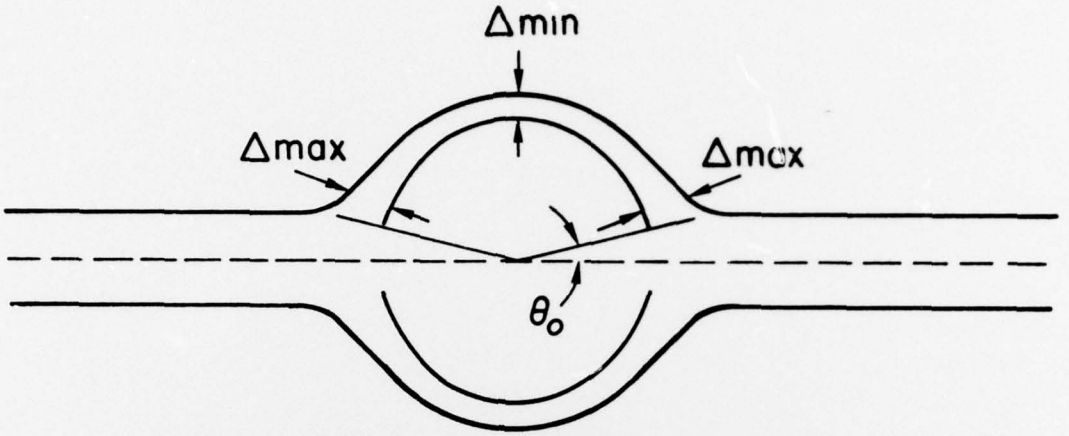

Fig. 3 - Expansion of bubble into constant density atmosphere. The development of the coupling shell is symmetric about Δmin. For coupling to occur $\theta > \theta_o \sim \sqrt{\Delta/R}$. Regions of earliest onset are demarked Δmax.

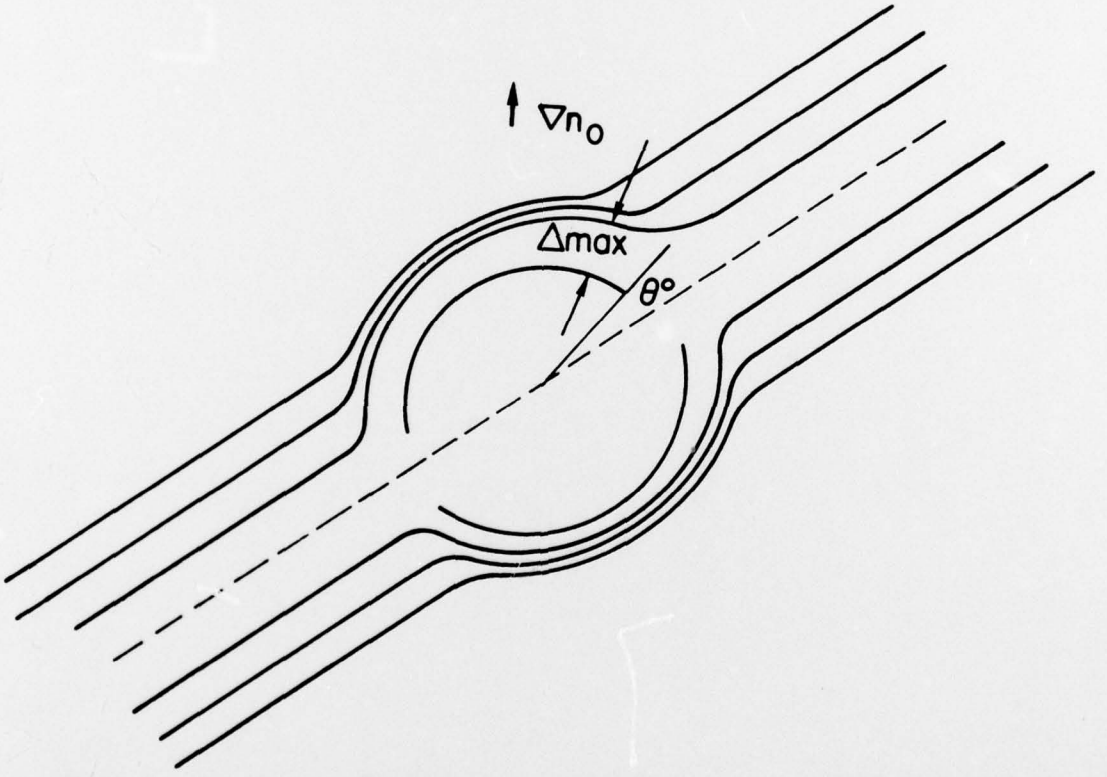

Fig. 4 - Expansion of bubble into atmosphere with density gradient directed upward and field lines directed obliquely to the gradient. Coupling shell has lost symmetry and Δmax is directed at an angle to both Δn_o and the field line. Region for earliest onset of the instability is demarked Δmax.

DISTRIBUTION LIST

DEPARTMENT OF DEFENSE

ASSISTANT SECRETARY OF DEFENSE
COMM, CMD, CONT & INTELL
WASHINGTON, D.C. 20301
01CY ATTN J. BABCOCK
01CY ATTN M. EPSTEIN

ASSISTANT TO THE SECRETARY OF DEFENSE
ATOMIC ENERGY
WASHINGTON, D.C. 20301
01CY ATTN EXECUTIVE ASSISTANT

DIRECTOR
COMMAND CONTROL TECHNICAL CENTER
PENTAGON RM BE 685
WASHINGTON, D.C. 20301
01CY ATTN C-650
01CY ATTN C-312 R. MASON

DIRECTOR
DEFENSE ADVANCED RSCH PROJ AGENCY
ARCHITECT BUILDING
1400 WILSON BLVD.
ARLINGTON, VA. 22209
01CY ATTN NUCLEAR MONITORING RESEARCH
01CY ATTN STRATEGIC TECH OFFICE

DEFENSE COMMUNICATION ENGINEER CENTER
1860 WIEHLE AVENUE
RESTON, VA. 22090
01CY ATTN CODE R820
01CY ATTN CODE R410 JAMES W. MCLEAN
01CY ATTN CODE R720 J. WORTHINGTON

DIRECTOR
DEFENSE COMMUNICATIONS AGENCY
WASHINGTON, D.C. 20305
(ADR CNWDI: ATTN CODE 240 FOR)

01CY ATTN CODE 1018

DEFENSE DOCUMENTATION CENTER
CAMERON STATION
ALEXANDRIA, VA. 22314
(12 COPIES IF OPEN PUBLICATION, OTHERWISE 2 COPIES)
12CY ATTN TC

DIRECTOR
DEFENSE INTELLIGENCE AGENCY
WASHINGTON, D.C. 20301
01CY ATTN DT-1B
01CY ATTN DB-4C E. O'FARRELL
01CY ATTN DIAAP A. WISE
01CY ATTN DIAST-5
01CY ATTN DT-1BZ R. MORTON
01CY ATTN HQ-TR J. STEWART
01CY ATTN W. WITTIG DC-7D

DIRECTOR
DEFENSE NUCLEAR AGENCY
WASHINGTON, D.C. 20305
01CY ATTN STVL
04CY ATTN TITL
01CY ATTN DDST
03CY ATTN RAAE

COMMANDER
FIELD COMMAND
DEFENSE NUCLEAR AGENCY
KIRTLAND AFB, NM 87115
01CY ATTN FCPR

DIRECTOR
INTERSERVICE NUCLEAR WEAPONS SCHOOL
KIRTLAND AFB, NM 87115
01CY ATTN DOCUMENT CONTROL

JOINT CHIEFS OF STAFF
WASHINGTON, D.C. 20301
01CY ATTN J-3 WWMCCS EVALUATION OFFICE

DIRECTOR
JOINT STRAT TGT PLANNING STAFF
OFFUTT AFB
OMAHA, NB 68113
01CY ATTN JLTW-2
01CY ATTN JPST G. GOETZ

CHIEF
LIVERMORE DIVISION FLD COMMAND DNA
DEPARTMENT OF DEFENSE
LAWRENCE LIVERMORE LABORATORY
P. O. BOX 808
LIVERMORE, CA 94550
01CY ATTN FCPRL

DIRECTOR
NATIONAL SECURITY AGENCY
DEPARTMENT OF DEFENSE
FT. GEORGE G. MEADE, MD 20755
01CY ATTN JOHN SKILLMAN R52
01CY ATTN FRANK LEONARD
01CY ATTN W14 PAT CLARK
01CY ATTN OLIVER H. BARTLETT W32
01CY ATTN R5

COMMANDANT
NATO SCHOOL (SHAPE)
APO NEW YORK 09172
01CY ATTN U.S. DOCUMENTS OFFICER

UNDER SECY OF DEF FOR RSCH & ENGRG
DEPARTMENT OF DEFENSE
WASHINGTON, D.C. 20301
01CY ATTN STRATEGIC & SPACE SYSTEMS (OS)

WWMCCS SYSTEM ENGINEERING ORG
WASHINGTON, D.C. 20305
01CY ATTN R. CRAWFORD

COMMANDER/DIRECTOR
ATMOSPHERIC SCIENCES LABORATORY
U.S. ARMY ELECTRONICS COMMAND
WHITE SANDS MISSILE RANGE, NM 88002
01CY ATTN DELAS-EO F. NILES

DIRECTOR
BMD ADVANCED TECH CTR
HUNTSVILLE OFFICE
P. O. BOX 1500
HUNTSVILLE, AL 35807
01CY ATTN ATC-T MELVIN T. CAPPS
01CY ATTN ATC-O W. DAVIES
01CY ATTN ATC-R DON RUSS

PROGRAM MANAGER
BMD PROGRAM OFFICE
5001 EISENHOWER AVENUE
ALEXANDRIA, VA 22333
01CY ATTN DACS-BMT J. SHEA

CHIEF C-E SERVICES DIVISION
U.S. ARMY COMMUNICATIONS CMD
PENTAGON RM 18269
WASHINGTON, D.C. 20310
01CY ATTN C-E-SERVICES DIVISION

COMMANDER
FRADCOM TECHNICAL SUPPORT ACTIVITY
DEPARTMENT OF THE ARMY
FORT MONMOUTH, N.J. 07703
01CY ATTN DRSEL-NL-RD H. BENNET
01CY ATTN DRSEL-PL-ENV H. BOMKE
01CY ATTN J. E. QUIGLEY

COMMANDER
NAVAL OCEAN SYSTEMS CENTER
SAN DIEGO, CA 92152
03CY ATTN CODE 532 W. MOLER
01CY ATTN CODE 0230 C. BAGGETT
01CY ATTN CODE 81 R. EASTMAN

DIRECTOR
NAVAL RESEARCH LABORATORY
WASHINGTON, D.C. 20375
01CY ATTN CODE 6700 TIMOTHY P. COFFEY
(25 CYS IF UNCLASS, 1 CY IF CLASS)
01CY ATTN CODE 6701 JACK D. BROWN
01CY ATTN CODE 6780 BRANCH HEAD (150 CYS IF UNCLASS, 1 CY IF CLASS)
01CY ATTN CODE 7500 HQ COMM DIR BRUCE WALD
01CY ATTN CODE 7550 J. DAVIS
01CY ATTN CODE 7580
01CY ATTN CODE 7551
01CY ATTN CODE 7555
01CY ATTN CODE 6730 E. MCLEAN
01CY ATTN CODE 7127 C. JOHNSON

COMMANDER
NAVAL SEA SYSTEMS COMMAND
WASHINGTON, D.C. 20362
01CY ATTN CAPT R. PITKIN

COMMANDER
NAVAL SPACE SURVEILLANCE SYSTEM
DAHLGREN, VA 22448
01CY ATTN CAPT J. H. BURTON

OFFICER-IN-CHARGE
NAVAL SURFACE WEAPONS CENTER
WHITE OAK, SILVER SPRING, MD 20910
01CY ATTN CODE F31

DIRECTOR
STRATEGIC SYSTEMS PROJECT OFFICE
DEPARTMENT OF THE NAVY
WASHINGTON, D.C. 20376
01CY ATTN NSP-2141
01CY ATTN NSSP-2722 FRED WIMBERLY

NAVAL SPACE SYSTEM ACTIVITY
P. O. BOX 92960
WORLDWAY POSTAL CENTER
LOS ANGELES, CALIF. 90009
01CY ATTN A. B. HAZZARD

HEADQUARTERS
ELECTRONIC SYSTEMS DIVISION/DC
DEPARTMENT OF THE AIR FORCE
HANSCOM AFB, MA 01731
01CY ATTN DOKC MAJ J. C. CLARK

[illegible]TR
[illegible] TECHNOLOGY DIVISION, AFSC
[illegible] ATTERSON AFB, OH 45433
[illegible]CY ATTN NICD LIBRARY
01CY ATTN ETDP B. BALLARD

COMMANDER
ROME AIR DEVELOPMENT CENTER, AFSC
GRIFFISS AFB, NY 13441
01CY ATTN DOC LIBRARY/TSLD
01CY ATTN OCSE V. COYNE

SAMSO/SZ
POST OFFICE BOX 92960
WORLDWAY POSTAL CENTER
LOS ANGELES, CA 90009
(SPACE DEFENSE SYSTEMS)
01CY ATTN SZJ

STRATEGIC AIR COMMAND/XPFS
OFFUTT AFB, NB 68113
01CY ATTN XPFS MAJ B. STEPHAN
01CY ATTN ADWATE MAJ BRUCE BAUER
01CY ATTN NRT
01CY ATTN DOK CHIEF SCIENTIST

SAMSO/YA
P. O. BOX 92960
WORLDWAY POSTAL CENTER
LOS ANGELES, CA 90009
01CY ATTN YAT CAPT L. BLACKWELDER

SAMSO/SK
P. O. BOX 92960
WORLDWAY POSTAL CENTER
LOS ANGELES, CA 90009
01CY ATTN SKA (SPACE COMM SYSTEMS) M. CLAVIN

SAMSO/MN
NORTON AFB, CA 92409
(MINUTEMAN)
01CY ATTN MNNL LTC KENNEDY

COMMANDER
ROME AIR DEVELOPMENT CENTER, AFSC
HANSCOM AFB, MA 01731
01CY ATTN EEP A. LORENTZEN

DEPARTMENT OF ENERGY

DEPARTMENT OF ENERGY
ALBUQUERQUE OPERATIONS OFFICE
P. O. BOX 5400
ALBUQUERQUE, NM 87115
01CY ATTN DOC CON FOR D. SHERWOOD

DEPARTMENT OF ENERGY
LIBRARY ROOM G-042
WASHINGTON, D.C. 20545
01CY ATTN DOC CON FOR A. LABOWITZ

EG&G, INC.
LOS ALAMOS DIVISION
P. O. BOX 809
LOS ALAMOS, NM 85544
01CY ATTN DOC CON FOR J. BREEDLOVE

UNIVERSITY OF CALIFORNIA
LAWRENCE LIVERMORE LABORATORY
P. O. BOX 808
LIVERMORE, CA 94550
01CY ATTN DOC CON FOR TECH INFO DEPT
01CY ATTN DOC CON FOR L-389 R. OTT
01CY ATTN DOC CON FOR L-31 R. HAGER
01CY ATTN DOC CON FOR L-46 F. SEWARD

LOS ALAMOS SCIENTIFIC LABORATORY
P. O. BOX 1663
LOS ALAMOS, NM 87545
01CY ATTN DOC CON FOR J. WOLCOTT
01CY ATTN DOC CON FOR R. F. TASCHEK
01CY ATTN DOC CON FOR E. JONES
01CY ATTN DOC CON FOR J. MALIK
01CY ATTN DOC CON FOR R. JEFFRIES
01CY ATTN DOC CON FOR J. ZINN
01CY ATTN DOC CON FOR P. KEATON
01CY ATTN DOC CON FOR D. WESTERVELT

SANDIA LABORATORIES
P. O. BOX 5800
ALBUQUERQUE, NM 87115
01CY ATTN DOC CON FOR J. MARTIN
01CY ATTN DOC CON FOR W. BROWN
01CY ATTN DOC CON FOR A. THORNBROUGH
01CY ATTN DOC CON FOR T. WRIGHT
01CY ATTN DOC CON FOR D. DAHLGREN
01CY ATTN DOC CON FOR 3141
01CY ATTN DOC CON FOR SPACE PROJECT DIV

SANDIA LABORATORIES
LIVERMORE LABORATORY
P. O. BOX 969
LIVERMORE, CA 94550
01CY ATTN DOC CON FOR B. MURPHEY
01CY ATTN DOC CON FOR T. COOK

OFFICE OF MILITARY APPLICATION
DEPARTMENT OF ENERGY
WASHINGTON, D.C. 20545
01CY ATTN DOC CON FOR D. GALE

OTHER GOVERNMENT

CENTRAL INTELLIGENCE AGENCY
ATTN RD/SI, RM 5G48, HQ BLDG
WASHINGTON, D.C. 20505
01CY ATTN OSI/PSID RM 5F 19

DEPARTMENT OF COMMERCE
NATIONAL BUREAU OF STANDARDS
WASHINGTON, D.C. 20234
(ALL CORRES: ATTN SEC OFFICER FOR)
01CY ATTN R. MOORE

DEPARTMENT OF TRANSPORTATION
OFFICE OF THE SECRETARY
TAD-44.1, ROOM 10402-B
400 7TH STREET, S.W.
WASHINGTON, D.C. 20590
01CY ATTN R. LEWIS
01CY ATTN R. DOHERTY

INSTITUTE FOR TELECOM SCIENCES
NATIONAL TELECOMMUNICATIONS & INFO ADMIN
BOULDER, CO 80303
01CY ATTN A. JEAN (UNCLASS ONLY)
01CY ATTN W. UTLAUT
01CY ATTN D. CROMBIE
01CY ATTN L. BERRY

NATIONAL OCEANIC & ATMOSPHERIC ADMIN
ENVIRONMENTAL RESEARCH LABORATORIES
DEPARTMENT OF COMMERCE
BOULDER, CO 80302
01CY ATTN R. GRUBB
01CY ATTN AERONOMY LAB G. REID

DEPARTMENT OF DEFENSE CONTRACTORS

AEROSPACE CORPORATION
P. O. BOX 92957
LOS ANGELES, CA 90009
01CY ATTN I. GARFUNKEL
01CY ATTN T. SALMI
01CY ATTN V. JOSEPHSON
01CY ATTN S. BOWER
01CY ATTN N. STOCKWELL
01CY ATTN D. OLSEN
01CY ATTN J. CARTER
01CY ATTN F. MORSE
01CY ATTN SMFA FOR PWW

ANALYTICAL SYSTEMS ENGINEERING CORP
5 OLD CONCORD ROAD
BURLINGTON, MA 01803
01CY ATTN RADIO SCIENCES

BERKELEY RESEARCH ASSOCIATES, INC.
P. O. BOX 983
BERKELEY, CA 94701
01CY ATTN J. WORKMAN

BOEING COMPANY, THE
P. O. BOX 3707
SEATTLE, WA 98124
01CY ATTN G. KEISTER
01CY ATTN D. MURRAY
01CY ATTN G. HALL
01CY ATTN J. KENNEY

CALIFORNIA AT SAN DIEGO, UNIV OF
IPAPS, B-019
LA JOLLA, CA 92093
01CY ATTN HENRY G. BOOKER

BROWN ENGINEERING COMPANY, INC.
CUMMINGS RESEARCH PARK
HUNTSVILLE, AL 35807
01CY ATTN ROMEO A. DELIBERIS

CHARLES STARK DRAPER LABORATORY, INC.
555 TECHNOLOGY SQUARE
CAMBRIDGE, MA 02139
01CY ATTN D. B. COX
01CY ATTN J. P. GILMORE

COMPUTER SCIENCES CORPORATION
6565 ARLINGTON BLVD
FALLS CHURCH, VA 22046
01CY ATTN H. BLANK
01CY ATTN JOHN SPOOR
01CY ATTN C. NAIL

COMSAT LABORATORIES
LINTHICUM ROAD
CLARKSBURG, MD 20734
01CY ATTN G. HYDE

CORNELL UNIVERSITY
DEPARTMENT OF ELECTRICAL ENGINEERING
ITHACA, NY 14850
01CY ATTN D. T. FARLEY JR

ELECTROSPACE SYSTEMS, INC.
BOX 1359
RICHARDSON, TX 75080
01CY ATTN H. LOGSTON
01CY ATTN SECURITY (PAUL PHILLIPS)

ESL INC.
495 JAVA DRIVE
SUNNYVALE, CA 94086
01CY ATTN J. ROBERTS
01CY ATTN JAMES MARSHALL
01CY ATTN C. W. PRETTIE

FORD AEROSPACE & COMMUNICATIONS CORP
3939 FABIAN WAY
PALO ALTO, CA 94303
01CY ATTN J. T. MATTINGLEY

GENERAL ELECTRIC COMPANY
SPACE DIVISION
VALLEY FORGE SPACE CENTER
GODDARD BLVD KING OF PRUSSIA
P. O. BOX 8555
PHILADELPHIA, PA 19101
01CY ATTN M. H. BORTNER SPACE SCI LAB

GENERAL ELECTRIC COMPANY
P. O. BOX 1122
SYRACUSE, NY 13201
01CY ATTN F. REIBERT

GENERAL ELECTRIC COMPANY
TEMPO-CENTER FOR ADVANCED STUDIES
816 STATE STREET (P.O. DRAWER QQ)
SANTA BARBARA, CA 93102
01CY ATTN DASIAC
01CY ATTN DON CHANDLER
01CY ATTN TOM BARRETT
01CY ATTN TIM STEPHANS
01CY ATTN WARREN S. KNAPP
01CY ATTN WILLIAM MCNAMARA
01CY ATTN B. GAMBILL
01CY ATTN MACK STANTON

COMMANDER
HARRY DIAMOND LABORATORIES
DEPARTMENT OF THE ARMY
2800 POWDER MILL ROAD
ADELPHI, MD 20783
(CNWDI-INNER ENVELOPE: ATTN: DELHD-RBH)
01CY ATTN DELHD-TI M. WEINER
01CY ATTN DELHD-RB R. WILLIAMS
01CY ATTN DELHD-NP F. WIMENITZ
01CY ATTN DELHD-NP C. MOAZED

COMMANDER
U.S. ARMY COMM-ELEC ENGRG INSTAL AGY
FT. HUACHUCA, AZ 85613
01CY ATTN CCC-EMEO GEORGE LANE

COMMANDER
U.S. ARMY FOREIGN SCIENCE & TECH CTR
220 7TH STREET, NE
CHARLOTTESVILLE, VA 22901
01CY ATTN DRXST-SD
01CY ATTN R. JONES

COMMANDER
U.S. ARMY MATERIEL DEV & READINESS CMD
5001 EISENHOWER AVENUE
ALEXANDRIA, VA 22333
01CY ATTN DRCLDC J. A. BENDER

COMMANDER
U.S. ARMY NUCLEAR AND CHEMICAL AGENCY
7500 BACKLICK ROAD
BLDG 2073
SPRINGFIELD, VA 22150
01CY ATTN LIBRARY

DIRECTOR
U.S. ARMY BALLISTIC RESEARCH LABS
ABERDEEN PROVING GROUND, MD 21005
01CY ATTN TECH LIB EDWARD BAICY

COMMANDER
U.S. ARMY SATCOM AGENCY
FT. MONMOUTH, NJ 07703
01CY ATTN DOCUMENT CONTROL

COMMANDER
U.S. ARMY MISSILE INTELLIGENCE AGENCY
REDSTONE ARSENAL, AL 35809
01CY ATTN JIM GAMBLE

DIRECTOR
U.S. ARMY TRADOC SYSTEMS ANALYSIS ACTIVITY
WHITE SANDS MISSILE RANGE, NM 88002
01CY ATTN ATAA-SA
01CY ATTN TCC/F. PAYAN JR.
01CY ATTN ATAA-TAC LTC J. HESSE

COMMANDER
NAVAL ELECTRONIC SYSTEMS COMMAND
WASHINGTON, D.C. 20360
01CY ATTN NAVALEX 034 T. HUGHES
01CY ATTN PME 117
01CY ATTN PME 117-T
01CY ATTN CODE 5011

COMMANDING OFFICER
NAVAL INTELLIGENCE SUPPORT CTR
4301 SUITLAND ROAD, BLDG. 5
WASHINGTON, D.C. 20390
01CY ATTN MR. DUBBIN STIC 12
01CY ATTN NISC-50
01CY ATTN CODE 5404 J. GALET

COMMANDER
NAVAL SURFACE WEAPONS CENTER
DAHLGREN LABORATORY
DAHLGREN, VA 22448
01CY ATTN CODE DF-14 R. BUTLER

COMMANDING OFFICER
NAVY SPACE SYSTEMS ACTIVITY
P.O. BOX 92960
WORLDWAY POSTAL CENTER
LOS ANGELES, CA. 90009
01CY ATTN CODE 52

OFFICE OF NAVAL RESEARCH
ARLINGTON, VA 22217
01CY ATTN CODE 465
01CY ATTN CODE 461
01CY ATTN CODE 402
01CY ATTN CODE 420
01CY ATTN CODE 421

COMMANDER
AEROSPACE DEFENSE COMMAND/DC
DEPARTMENT OF THE AIR FORCE
ENT AFB, CO 80912
01CY ATTN DC MR. LONG

COMMANDER
AEROSPACE DEFENSE COMMAND/XPD
DEPARTMENT OF THE AIR FORCE
ENT AFB, CO 80912
01CY ATTN XPDQQ
01CY ATTN XP

AIR FORCE GEOPHYSICS LABORATORY
HANSCOM AFB, MA 01731
01CY ATTN OPR HAROLD GARDNER
01CY ATTN OPR-1 JAMES C. ULWICK
01CY ATTN LKB KENNETH S. W. CHAMPION
01CY ATTN OPR ALVA T. STAIR
01CY ATTN PHP JULES AARONS
01CY ATTN PHD JURGEN BUCHAU
01CY ATTN PHD JOHN P. MULLEN

AF WEAPONS LABORATORY
KIRTLAND AFB, NM 87117
01CY ATTN SUL
01CY ATTN CA ARTHUR H. GUENTHER
01CY ATTN DYC CAPT J. BARRY
01CY ATTN DYC JOHN M. KAMM
01CY ATTN DYT CAPT MARK A. FRY
01CY ATTN DES MAJ GARY GANONG
01CY ATTN DYC J. JANNI

AFTAC
PATRICK AFB, FL 32925
01CY ATTN TF/MAJ WILEY
01CY ATTN TN

AIR FORCE AVIONICS LABORATORY
WRIGHT-PATTERSON AFB, OH 45433
01CY ATTN AAD WADE HUNT
01CY ATTN AAD ALLEN JOHNSON

DEPUTY CHIEF OF STAFF
RESEARCH, DEVELOPMENT, & ACQ
DEPARTMENT OF THE AIR FORCE
WASHINGTON, D.C. 20330
01CY ATTN AFRDQ

HEADQUARTERS
ELECTRONIC SYSTEMS DIVISION/XR
DEPARTMENT OF THE AIR FORCE
HANSCOM AFB, MA 01731
01CY ATTN XR J. DEAS

HEADQUARTERS
ELECTRONIC SYSTEMS DIVISION/YSEA
DEPARTMENT OF THE AIR FORCE
HANSCOM AFB, MA 01731
01CY ATTN YSEA

GENERAL ELECTRIC TECH SERVICES CO., INC.
HMES
COURT STREET
SYRACUSE, NY 13201
01CY ATTN G. MILLMAN

GENERAL RESEARCH CORPORATION
SANTA BARBARA DIVISION
P. O. BOX 6770
SANTA BARBARA, CA 93111
01CY ATTN JOHN ISE JR
01CY ATTN JOEL GARBARINO

GEOPHYSICAL INSTITUTE
UNIVERSITY OF ALASKA
FAIRBANKS, AK 99701
(ALL CLASS ATTN: SECURITY OFFICER)
01CY ATTN T. N. DAVIS (UNCL ONLY)
01CY ATTN NEAL BROWN (UNCL ONLY)
01CY ATTN TECHNICAL LIBRARY

GTE SYLVANIA, INC.
ELECTRONICS SYSTEMS GRP-EASTERN DIV
77 A STREET
NEEDHAM, MA 02194
01CY ATTN MARSHAL CROSS

ILLINOIS, UNIVERSITY OF
DEPARTMENT OF ELECTRICAL ENGINEERING
URBANA, IL 61803
01CY ATTN K. YEH

ILLINOIS, UNIVERSITY OF
107 COBLE HALL
801 S. WRIGHT STREET
URBANA, IL 60680
(ALL CORRES ATTN SECURITY SUPERVISOR FOR)
01CY ATTN K. YEH

INSTITUTE FOR DEFENSE ANALYSES
400 ARMY-NAVY DRIVE
ARLINGTON, VA 22202
01CY ATTN J. M. AEIN
01CY ATTN ERNEST BAUER
01CY ATTN HANS WOLFHARD
01CY ATTN JOEL BENGSTON

HSS, INC.
2 ALFRED CIRCLE
BEDFORD, MA 01730
01CY ATTN DONALD HANSEN

INTL TEL & TELEGRAPH CORPORATION
500 WASHINGTON AVENUE
NUTLEY, NJ 07110
01CY ATTN TECHNICAL LIBRARY

JAYCOR
1401 CAMINO DEL MAR
DEL MAR, CA 92014
01CY ATTN S. R. GOLDMAN

JOHNS HOPKINS UNIVERSITY
APPLIED PHYSICS LABORATORY
JOHNS HOPKINS ROAD
LAUREL, MD 20810
01CY ATTN DOCUMENT LIBRARIAN
01CY ATTN THOMAS POTEMRA
01CY ATTN JOHN DASSOULAS

LOCKHEED MISSILES & SPACE CO INC
P. O. BOX 504
SUNNYVALE, CA 94088
01CY ATTN DEPT 60-12
01CY ATTN D. R. CHURCHILL

LOCKHEED MISSILES AND SPACE CO INC
3251 HANOVER STREET
PALO ALTO, CA 94304
01CY ATTN MARTIN WALT DEPT 52-10
01CY ATTN RICHARD G. JOHNSON DEPT 52-12
01CY ATTN W. L. IMHOF DEPT 52-12

KAMAN SCIENCES CORP
P. O. BOX 7463
COLORADO SPRINGS, CO 80933
01CY ATTN T. MEAGHER

LINKABIT CORP
10453 ROSELLE
SAN DIEGO, CA 92121
01CY ATTN IRWIN JACOBS

LOWELL RSCH FOUNDATION, UNIVERSITY OF
450 AIKEN STREET
LOWELL, MA 01854
01CY ATTN K. BIBL

M.I.T. LINCOLN LABORATORY
P. O. BOX 73
LEXINGTON, MA 02173
01CY ATTN DAVID M. TOWLE
01CY ATTN P. WALDRON
01CY ATTN L. LOUGHLIN
01CY ATTN D. CLARK

MARTIN MARIETTA CORP
ORLANDO DIVISION
P. O. BOX 5837
ORLANDO, FL 32805
01CY ATTN R. HEFFNER

MCDONNELL DOUGLAS CORPORATION
5301 BOLSA AVENUE
HUNTINGTON BEACH, CA 92647
01CY ATTN N. HARRIS
01CY ATTN J. MOULE
01CY ATTN GEORGE MROZ
01CY ATTN W. OLSON
01CY ATTN R. W. HALPRIN
01CY ATTN TECHNICAL LIBRARY SERVICES

MISSION RESEARCH CORPORATION
735 STATE STREET
SANTA BARBARA, CA 93101
01CY ATTN P. FISCHER
01CY ATTN W. F. CREVIER
01CY ATTN STEVEN L. GUTSCHE
01CY ATTN D. SAPPENFIELD
01CY ATTN R. BOGUSCH
01CY ATTN R. HENDRICK
01CY ATTN RALPH KILB
01CY ATTN DAVE SOWLE
01CY ATTN F. FAJEN
01CY ATTN M. SCHEIBE
01CY ATTN CONRAD L. LONGMIRE
01CY ATTN WARREN A. SCHLUETER

MITRE CORPORATION, THE
P. O. BOX 208
BEDFORD, MA 01730
01CY ATTN JOHN MORGANSTERN
01CY ATTN G. HARDING
01CY ATTN C. E. CALLAHAN

MITRE CORP
WESTGATE RESEARCH PARK
1820 DOLLY MADISON BLVD
MCLEAN, VA 22101
01CY ATTN W. HALL
01CY ATTN W. FOSTER

PACIFIC-SIERRA RESEARCH CORP
1456 CLOVERFIELD BLVD.
SANTA MONICA, CA 90404
01CY ATTN E. C. FIELD JR

PENNSYLVANIA STATE UNIVERSITY
IONOSPHERE RESEARCH LAB
318 ELECTRICAL ENGINEERING EAST
UNIVERSITY PARK, PA 16802
(NO CLASSIFIED TO THIS ADDRESS)
01CY ATTN IONOSPHERIC RESEARCH LAB

PHOTOMETRICS, INC.
442 MARRETT ROAD
LEXINGTON, MA 02173
01CY ATTN IRVING L. KOFSKY

PHYSICAL DYNAMICS INC.
P. O. BOX 3027
BELLEVUE, WA 98009
01CY ATTN E. J. FREMOUW

PHYSICAL DYNAMICS INC.
P. O. BOX 1069
BERKELEY, CA 94701
01CY ATTN A. THOMPSON

R & D ASSOCIATES
P. O. BOX 9695
MARINA DEL REY, CA 90291
01CY ATTN FORREST GILMORE
01CY ATTN BRYAN GABBARD
01CY ATTN WILLIAM B. WRIGHT JR
01CY ATTN ROBERT F. LELEVIER
01CY ATTN WILLIAM J. KARZAS
01CY ATTN H. ORY
01CY ATTN C. MACDONALD
01CY ATTN R. TURCO

RAND CORPORATION, THE
1700 MAIN STREET
SANTA MONICA, CA 90406
01CY ATTN CULLEN CRAIN
01CY ATTN ED BEDROZIAN

RIVERSIDE RESEARCH INSTITUTE
80 WEST END AVENUE
NEW YORK, NY 10023
01CY ATTN VINCE TRAPANI

SCIENCE APPLICATIONS, INC.
P. O. BOX 2351
LA JOLLA, CA 92038
01CY ATTN LEWIS M. LINSON
01CY ATTN DANIEL A. HAMLIN
01CY ATTN D. SACHS
01CY ATTN E. A. STRAKER
01CY ATTN CURTIS A. SMITH
01CY ATTN JACK MCDOUGALL

RAYTHEON CO.
528 BOSTON POST ROAD
SUDBURY, MA 01776
01CY ATTN BARBARA ADAMS

SCIENCE APPLICATIONS, INC.
HUNTSVILLE DIVISION
2109 W. CLINTON AVENUE
SUITE 700
HUNTSVILLE, AL 35805
01CY ATTN DALE H. DIVIS

SCIENCE APPLICATIONS, INCORPORATED
8400 WESTPARK DRIVE
MCLEAN, VA 22101
01CY ATTN J. COCKAYNE

SCIENCE APPLICATIONS, INC.
80 MISSION DRIVE
PLEASANTON, CA 94566
01CY ATTN SZ

SRI INTERNATIONAL
333 RAVENSWOOD AVENUE
MENLO PARK, CA 94025
01CY ATTN DONALD NEILSON
01CY ATTN ALAN BURNS
01CY ATTN G. SMITH
01CY ATTN L. L. COBB
01CY ATTN DAVID A. JOHNSON
01CY ATTN WALTER G. CHESNUT
01CY ATTN CHARLES L. RINO
01CY ATTN WALTER JAYE
01CY ATTN M. BARON
01CY ATTN RAY L. LEADABRAND
01CY ATTN G. CARPENTER
01CY ATTN G. PRICE
01CY ATTN J. PETERSON
01CY ATTN R. HAKE, JR.
01CY ATTN V. GONZALES
01CY ATTN D. MCDANIEL

TECHNOLOGY INTERNATIONAL CORP
75 WIGGINS AVENUE
BEDFORD, MA 01730
01CY ATTN W. P. BOQUIST

TRW DEFENSE & SPACE SYS GROUP
ONE SPACE PARK
REDONDO BEACH, CA 90278
01CY ATTN R. K. PLEBUCH
01CY ATTN S. ALTSCHULER
01CY ATTN D. DEE

VISIDYNE, INC.
19 THIRD AVENUE
NORTH WEST INDUSTRIAL PARK
BURLINGTON, MA 01803
01CY ATTN CHARLES HUMPHREY
01CY ATTN J. W. CARPENTER